Development 130, 3379-3390

doi:10.1242/dev.00555

Fgf3 and *Fgf10* are required for mouse otic placode induction

Tracy J. Wright and Suzanne L. Mansour*

Department of Human Genetics, University of Utah, Salt Lake City, UT 84112-5330, USA
*Author for correspondence (e-mail: suzi.mansour@genetics.utah.edu)

Accepted 23 April 2003

SUMMARY

The inner ear, which contains the sensory organs specialised for audition and balance, develops from an ectodermal placode adjacent to the developing hindbrain. Tissue grafting and recombination experiments suggest that placodal development is directed by signals arising from the underlying mesoderm and adjacent neurectoderm. In mice, *Fgf3* is expressed in the neurectoderm prior to and concomitant with placode induction and otic vesicle formation, but its absence affects only the later stages of otic vesicle morphogenesis. We show here that mouse *Fgf10* is expressed in the mesenchyme underlying the prospective otic placode. Embryos lacking both *Fgf3* and *Fgf10* fail to form otic vesicles and have aberrant patterns of otic marker gene expression, suggesting that FGF signals are required for otic placode induction and that these signals emanate from both the hindbrain and mesenchyme. These signals are likely to act directly on the ectoderm, as double mutant embryos showed normal patterns of gene expression in the hindbrain. Cell proliferation and survival were not markedly affected in double mutant embryos, suggesting that the major role of FGF signals in otic induction is to establish normal patterns of gene expression in the prospective placode. Finally, examination of embryos carrying three out of the four mutant *Fgf* alleles revealed intermediate phenotypes, suggesting a quantitative requirement for FGF signalling in otic vesicle formation.

Key words: Fibroblast growth factor, Otic, Placode, Inner ear, Induction, Mouse mutant

INTRODUCTION

The inner ear, which contains the sensory organs specialised for audition and balance, develops from placodal ectoderm located adjacent to the developing hindbrain. Otic development is first apparent morphologically in the mouse when the surface ectoderm in the vicinity of rhombomeres (r) 5 and 6 thickens at the 4-13 somite stages to form the otic placode (Anniko and Wikstrom, 1984; Sulik and Cotanche, 1995; Rinkwitz et al., 2001; Kiernan et al., 2002). The placode subsequently invaginates during the 13-20 somite stages and forms a closed vesicle by 21-29 somites (Kiernan et al., 2002). The otic epithelium then initiates cellular differentiation and morphogenesis, which ultimately results in the exquisitely complex inner ear.

Transplantation studies in amphibia and avians have established that the region of surface ectoderm competent to form an otic vesicle is initially quite large (for reviews, see Torres and Giraldez, 1998; Baker and Bronner-Fraser, 2001; Noramly and Grainger, 2002). When quail ectoderm from the midbrain or somitic region in 1-6 somite embryos is grafted in place of presumptive chick otic ectoderm, it responds to inductive signals by expressing otic markers and by forming an ectopic vesicle. This competency declines rapidly with age and by 10 somites neither midbrain nor somitic ectoderm is competent to express otic markers or to contribute to the developing otic placode. Only the ectoderm near the hindbrain maintains these abilities (Groves and Bronner-Fraser, 2000). Therefore, as development proceeds, the region of otic competency becomes progressively restricted and the placodal tissue adjacent to the hindbrain becomes specified for an otic fate.

Tissue recombination experiments as well as genetic depletion and ablation studies in zebrafish and mice suggest that placodal development is directed by signals arising from the underlying mesenchyme and the adjacent neurectoderm (Baker and Bronner-Fraser, 2001; Kiernan et al., 2002). Co-culture of chick stage 7 mesendoderm that will underlie the presumptive otic placode with stage 5 anterior cephalic ectoderm induces the expression of otic markers in the ectoderm. By stage 9^{+}, the equivalent mesoderm only induces otic markers when adjacent neurectoderm is also included in the culture (Ladher et al., 2000). Furthermore, there are many examples of mouse and zebrafish mutants with hindbrain abnormalities that also have inner ear abnormalities. For example, the *kreisler* mutant mouse and the *valentino* mutant zebrafish, which carry mutations in orthologous hindbrain-expressed transcription factors, have otic defects that are secondary to disruption of r5 and r6 (Frohman et al., 1993; Cordes and Barsh, 1994; McKay et al., 1994; Moens et al., 1998).

The molecular identities of signals responsible for otic placode induction are the subject of intense interest. In the chick, mesodermal Fibroblast growth factor (*Fgf)19* and neurectodermal *Wnt8c* have the spatio-temporal expression patterns appropriate for otic inducers. Simultaneous

application of these factors to cultured chick anterior ectoderm elicits expression of a variety of otic markers, including *Fgf3* (Ladher et al., 2000). Mouse *Fgf15*, the presumed ortholog of chick and human *FGF19* (Ornitz and Itoh, 2001), however, is not expressed in the mesenchyme underlying the otic placode and *Fgf15* mutants do not have otic abnormalities, suggesting that this FGF is likely not to function as a uniquely necessary otic inducer in mice (T.J.W. and S.L.M., unpublished).

Fgf3, which in mice and chicks is normally expressed in a hindbrain domain that narrows to r5 and r6, and also in prospective otic ectoderm (Wilkinson et al., 1988; Mahmood et al., 1995; Mahmood et al., 1996; McKay et al., 1996), has also been proposed as an otic inducer (Represa et al., 1991). Indeed, ectopic expression of *Fgf3* in chick embryos induces the formation of small otic-like vesicles (Vendrell et al., 2000; Adamska et al., 2001), suggesting that *Fgf3* expression may be sufficient to promote otic vesicle formation.

Genetic depletion and ablation studies in zebrafish and mice reveal a more complex picture of the requirement for *Fgf* genes in otic development. Depletion of FGF3 by injection of *Fgf3* morpholinos into wild-type zebrafish embryos causes a reduction in otic vesicle size very similar to that seen in *ace* (*Fgf8*) mutants (Leger and Brand, 2002). Simultaneous depletion of both FGF3 and FGF8 by injection of both morpholinos into wild-type embryos or injection of *Fgf3* morpholinos into *ace* mutants blocks otic vesicle formation in most treated embryos, demonstrating that these two FGFs have redundant roles in zebrafish otic placode induction (Phillips et al., 2001; Leger and Brand, 2002; Maroon et al., 2002). In this species, however, both *Fgf3* and *Fgf8* are expressed in r4 and the otic defects seen in embryos lacking both FGFs are accompanied by severe abnormalities of hindbrain patterning (Maves et al., 2002; Walshe et al., 2002). Thus it is not clear whether FGF3 and FGF8 both signal directly to the prospective otic placode, or whether one or both factors are instead required for expression of the otic inducer(s) by the hindbrain. As *Fgf8* is not expressed in the mouse hindbrain (Crossley and Martin, 1995) (T.J.W. and S.L.M., unpublished) its function (if any) with respect to otic placode induction is likely to be different to that of zebrafish *Fgf8*. Unfortunately, mouse *Fgf8* null mutants die of severe gastrulation defects prior to the initiation of otic development (Sun et al., 1999). Therefore, potential roles for *Fgf8* in mouse otic development have not yet been established.

Genetic ablation of *Fgf3* expression in mice does affect ear development, but the reported effects initiate after formation of the otic vesicle and are confined to the later stages of vesicle morphogenesis. The defects, moreover, have incomplete penetrance and variable expressivity, suggestive of redundancy in the FGF signalling system during otic development (Mansour et al., 1993). In support of this idea, disruption of *Fgf10*, which is expressed in the developing otic cup and its neuronal derivatives (Pirvola et al., 2000), also causes morphogenetic and innervation abnormalities of otic development (Ohuchi et al., 2000; Pauley et al., 2003). Furthermore, ectopic expression of a secreted, dominant-negative form of the IgIIIb isoform of FGF receptor 2 (FGFR2b), which is the high-affinity receptor for FGFs-3, -7 and -10 (Ornitz et al., 1996; Igarashi et al., 1998), has effects on otic vesicle development that appear to be more severe than those of either *Fgf3* or *Fgf10* single mutants (Celli et al., 1998). Finally, specific elimination of the FGFR2b isoform by targeted mutagenesis of the exon encoding the IgIIIb splice variant causes highly penetrant otic abnormalities that are similar to those expected from an additive combination of the *Fgf3* and *Fgf10* mutant phenotypes (Pirvola et al., 2000).

We show here that mouse *Fgf10* is expressed in the mesenchyme underlying the prospective otic placode. To uncover potential redundancy between *Fgf3* and *Fgf10* during early otic development we generated double mutant embryos. These embryos lacked otic vesicles and had aberrant patterns of otic placode marker gene expression, suggesting that FGF3 and FGF10 signals are required redundantly for otic placode induction and that these signals emanate from both the hindbrain and mesenchyme. These signals are likely to act directly on the prospective otic ectoderm, as double mutant embryos showed normal patterns of gene expression in the hindbrain. There were no major effects on cell proliferation or survival in double mutant embryos, suggesting that the major role of FGF signalling in otic induction is to establish appropriate patterns of gene expression in the placode. In addition, examination of otic vesicles in embryos carrying three of four possible mutant *Fgf* alleles revealed intermediate phenotypes that could be distinguished both from each other as well as from embryos carrying two or four mutant alleles. We suggest that an FGF3 gradient may explain the quantitative and unequal requirement for these two FGFs in otic development.

MATERIALS AND METHODS

Mice

The targeted $Fgf3^{neo}$ and $Fgf10^{neo}$ mutant strains have been described (Mansour et al., 1993; Min et al., 1998). Animals heterozygous for each mutation were bred to generate double heterozygotes, which were intercrossed to generate embryos of all nine possible genotypes. Genotypes were determined using PCR amplification of yolk sac or tail DNA (McMahon et al., 1990). PCR analysis was performed in 10 μl reactions amplified in an air thermal cycler (Idaho Technologies) for 35 cycles of 0 seconds at 94°C, 0 seconds at 64°C (*Fgf3*) or 60°C (*Fgf10*) and 30 seconds at 72°C. The sequences of the *Fgf3* primers were: 5′ primer, 5′-GGATGGGCCTGATCTGGCTTC-3′; 3′ primer, 5′-GAGGTGCTCGTAAACGCCACC-3′; *Neo* primer, 5′-GCCTG-CTTGCCGAATATCATGG-3′. The sequences of the *Fgf10* primers were: 5′ primer, 5′-CATTGTGCCTCAGCCTTTCCC-3′; 3′ primer, 5′-CGACAGTCTTCATTCTTGGTCC-3′; *Neo* primer, 5′-CACCAA-AGAACGGAGCCGGTTG-3′.

In situ hybridisation

Embryos were isolated on the indicated days following detection of a vaginal plug. Controls demonstrating the standard expression patterns of *Fgf3*, *Fgf10*, *Fgfr2IgIIIb* and *Fgfr1* were performed using wild-type CD-1 embryos. Control embryos for otic marker gene expression studies came from the intercross litters and were matched to the mutant embryos by somite number. Digoxigenin-labelled probes were prepared, hybridised to the embryos and detected as described (Henrique et al., 1995). cDNAs used to prepare probes for *Fgf3* (Manley and Capecchi, 1995), *Fgf10* (Xu et al., 1998), *Fgfr2IgIIIb* (Orr-Urtreger et al., 1993), *Pax2* (Dressler et al., 1990), *Dlx5* (Depew et al., 1999), *Gbx2* (Wassarman et al., 1997), *Pax8* (Plachov et al., 1990), *Hoxb1* (Carpenter et al., 1993), *Krox20* (Carpenter et al., 1993) and *kr* (Cordes and Barsh, 1994) have been described in the cited publications. A probe for the 3′ UTR of *Fgfr1* was generated by cloning a PCR-amplified DNA fragment (bp 2408-2910 of cDNA

clone 3830408H21, GenBank accession number AK028354). The sequences of the PCR primers were: 5′ primer, 5′-ACCCTGTCC-CCAGTTTTCTCC-3′; 3′ primer, 5′-ACCAGGCAGGTATTTGGT-CA-3′. The product was cloned into pCRII (Invitrogen) and an antisense probe was generated by digesting the clone with Xho I and transcribing with Sp6 RNA polymerase.

Otic vesicle development was analysed at E9.5 using the marker genes *Dlx5* and *Pax2* (*n*=3 double mutants; *n*=4 *Fgf3*$^{-/-}$;*Fgf10*$^{+/-}$; *n*=4 *Fgf3*$^{+/-}$;*Fgf10*$^{-/-}$; *n*=5 *Fgf3*$^{-/-}$; *n*=4 *Fgf10*$^{-/-}$) and otic placode induction was analysed at E8.5 using *Dlx5*, *Pax2*, *Pax8* and *Gbx2* (*n*=6 double mutants). Hindbrain development was analysed using the molecular markers *Krox20*, *MafB/kr* and *HoxB1* (*n*=4 double mutants).

Whole mount detection of mitosis and apoptosis

To detect proliferating cells, embryos (*n*=2 controls, *n*=2 double mutants) were prepared and stained with an antibody directed against phosphorylated histone H3 as described (Gavalas et al., 2001). Whole mount detection of apoptosis was performed using the TUNEL method as described previously (*n*=3 controls, *n*=3 double mutants) (Maden et al., 1997; Graham, 1999). Following staining and observation of whole mounts, embryos were cryosectioned and sections containing the otic tissues were identified using anatomical markers. Phosphohistone H3-expressing cells or apoptotic cells were counted in the otic ectoderm, neurectoderm and the mesenchyme underlying the otic ectoderm of double heterozygote and double mutant embryos. As a control, mitotic or apoptotic cells were counted in the heart fields, which were unaffected in double mutant embryos. No consistent differences were identified between genotypes, and the sections shown in Fig. 5 illustrate the presence of mitotic or apoptotic cells in all the tissues relevant to otic induction.

Cryosectioning

Embryos stained for analysis of gene or protein expression were cryoprotected in sucrose and sectioned at 14 μm using a Leica cryostat as described (Stark et al., 2000).

Photography and size measurements

Whole embryos were photographed using a Zeiss SV-11 dissecting microscope fitted with a digital camera (Kodak MDS120 or MDS240). Sections were photographed using a Zeiss Axioscop fitted with DIC optics and a digital camera (AxioCam).

To compare the relative sizes of otic vesicles between embryos of different genotypes, we first found the central section taken through each vesicle of three E9.5 embryos of each genotype (*n*=6 ears and eyes) and then measured the areas of both the otic and the optic vesicles. To account for differences in staging of the embryos, we calculated the ratio of the otic vesicle area to the optic vesicle area (which is not affected by the *Fgf* mutations). To compare the positions of the otic vesicles in different embryos, the vertical distance from the dorsal surface of the neural tube to the dorsal surface of the otic vesicle was measured and compared to the dorsoventral length of the neural tube. All areas and lengths were determined by using the measurement functions in the AxioCam software package (Zeiss).

RESULTS

Fgf3, *Fgf10*, *Fgfr2IgIIIb* and *Fgfr1* have spatial and temporal patterns of expression that are consistent with roles in otic placode induction

Whole mount RNA in situ hybridisation followed by inspection of cryosections was used to determine the normal spatial and temporal expression patterns of *Fgf3* and *Fgf10* in early somite stage mouse embryos (Fig. 1). *Fgf3* was expressed in the hindbrain neurectoderm and in the presumptive otic ectoderm of embryos having as few as 3 somites (Fig. 1A,B). Expression of *Fgf3* in the otic placode was reduced relative to that in the neurectoderm by 12 somites (Fig. 1C,D). As previously described (Mahmood et al., 1996; McKay et al., 1996), neurectodermal expression of *Fgf3* persisted beyond 12 somites and was restricted primarily to r5 and r6 through otic vesicle formation at E 9.5 (data not shown).

Fgf10 transcripts were detected in mesenchyme underlying presumptive otic ectoderm initiating at or before formation of the first somite (Fig. 1E,F). Mesenchymal expression of *Fgf10* was still evident at 7 somites, at which time weak expression of *Fgf10* initiated in neurectoderm (Fig. 1G,H). By E8.75, the

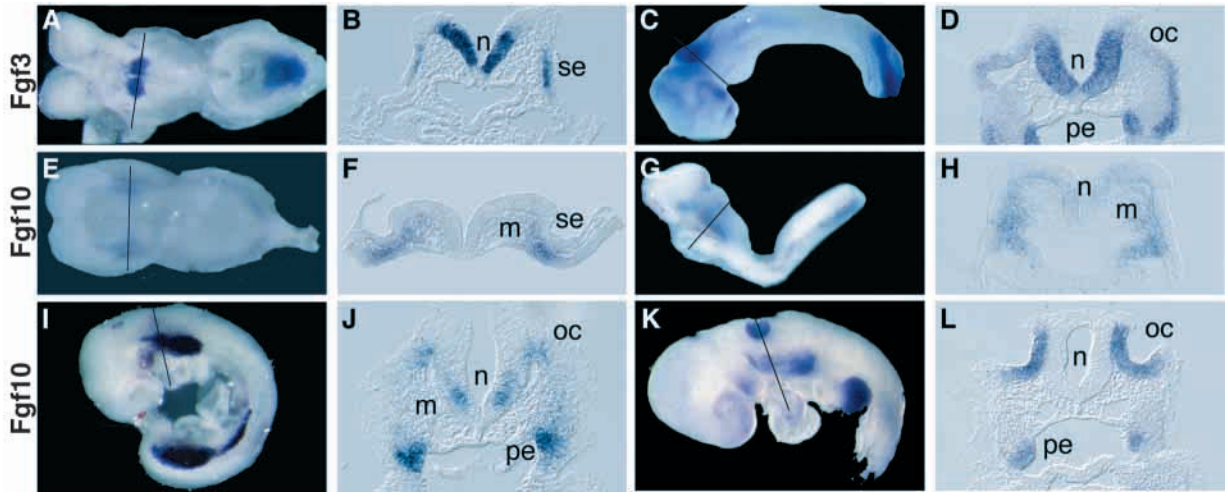

Fig. 1. *Fgf3* and *Fgf10* are expressed in sites relevant to early otic development. Whole mount embryos were probed with labelled cDNA for *Fgf3* (A,C) and *Fgf10* (E,G,I,K) and sectioned in the transverse plane. A section taken through the otic region (the plane is indicated by a line through each embryo) is shown in the panel to the right of each whole embryo. Rostral is to the left. *Fgf3* is expressed in the developing neurectoderm (n) and surface ectoderm (se) from 3 (A,B) to 12 (C,D) somites. *Fgf10* is expressed in the mesenchyme (m) that underlies the otic ectoderm at zero somites (E,F), 7 somites (G,H) and at E8.75 (I,J). By E9.0, *Fgf10* expression is induced in the otic cup (oc) (K,L). *Fgf10* transcripts can also be detected in the neurectoderm (G-J) and the pharyngeal endoderm (pe) (J,L).

level of *Fgf10* transcripts in mesenchyme diminished and expression in neurectoderm was restricted to the ventral domain (Fig. 1I,J). As also described by Pirvola et al. (Pirvola et al., 2000), *Fgf10* was expressed throughout the E9.0 otic cup (Fig. 1K,L) and E9.5 otic vesicle (data not shown), before becoming restricted to the delaminating and migrating neuroblasts of the eighth ganglion at E10.5 (data not shown).

If FGF3 and/or FGF10 signal to the otic ectoderm, an appropriate receptor should be present in that tissue. Of the seven major FGF receptor isoforms, both FGF3 and FGF10 bind with highest affinity to and signal most strongly through the IgIIIb isoform of FGFR2 (Ornitz et al., 1996; Igarashi et al., 1998). Therefore, we determined the early expression pattern of *Fgfr2b* by hybridising an isoform-specific probe to whole embryos (Fig. 2A-H). At 3 and 6 somites, *Fgfr2b* transcripts were found in the neurectoderm, extending along most of the anteroposterior axis of the embryo (Fig. 2A-D). To confirm that these transcripts were expressed in the hindbrain adjacent to presumptive otic ectoderm, we hybridized 2-8 somite embryos with a mixture of the probes for *Fgfr2b* and *Pax2*, a marker of otic ectoderm. In all cases, transverse sections exhibiting *Pax2* expression in the ectoderm also showed *Fgfr2b* expression in the neurectoderm (data not shown). Beginning at 8 somites, and coincident with ectodermal thickening, *Fgfr2b* transcripts were detected throughout the otic placode (Fig. 2E,F). This expression persisted through otic cup invagination in embryos with 16 somites (Fig. 2G,H). At this stage, *Fgfr2b* transcripts in neurectoderm were restricted to the most dorsal region (Fig. 2H). By E9.5, *Fgfr2b* transcripts in the otic vesicle and the neurectoderm were restricted to the dorsal domain (data not shown).

FGF3 and FGF10 are also capable of binding to and signalling through the IgIIIb isoform of FGFR1, albeit with lower affinity and activity than with FGFR2b (Ornitz et al., 1996; Igarashi et al., 1998). We were unable to reliably detect expression of *Fgfr1b* during the early stages of otic placode development using the small isoform-specific probe. A larger probe that detects both *Fgfr1b* and *Fgfr1c* transcripts, however, revealed low levels of *Fgfr1* expression in a pattern similar to that of *Fgfr2b* in early somite stage embryos (Fig. 2I-L). Specifically, *Fgfr1* was expressed in the neurectoderm of preplacodal embryos (Fig. 2I,J). Initiation of *Fgfr1* expression in the ectoderm coincided with thickening of the otic placode (Fig. 2K,L). During development, the 'b' isoforms of FGF receptors are generally epithelial, whereas the 'c' isoforms are usually mesenchymal (Orr-Urtreger et al., 1993; Kettunen et al., 1998). Thus we suppose that the *Fgfr1* signal detected in ectoderm probably represents expression of *Fgfr1b*. Therefore, *Fgf3*, *Fgf10* and *Fgfr2b* and *Fgfr1*, presumably the 'b' isoform, are expressed at the appropriate times and places to participate in otic placode induction.

Embryos homozygous for null mutations in both *Fgf3* and *Fgf10* do not develop otic vesicles

To determine whether *Fgf3* and *Fgf10* play redundant roles in otic placode induction, embryos lacking both *Fgf3* and *Fgf10* were generated by intercrossing mice that were heterozygous for null alleles of both genes. One-thousand two-hundred and sixty-nine embryos were harvested between E8 and E10.5 and all genotypes, including the double mutant, were obtained in the numbers expected for segregation of two unlinked recessive mutations (Table 1). Thus, early lethality did not compromise the analysis of the double mutant phenotype. Compared with double heterozygote control embryos at E10.5, double mutant embryos lacked limbs and had short dorsally curved tails (Fig.

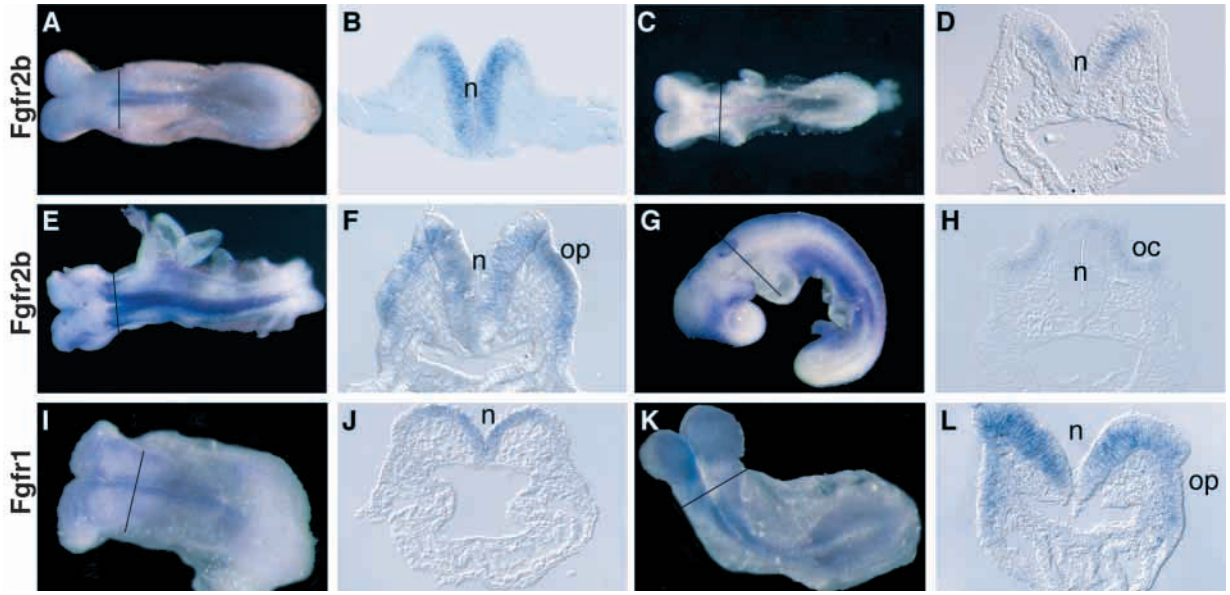

Fig. 2. *Fgfr2b* and *Fgfr1* are expressed in prospective otic placode. Whole mount embryos were probed with labelled cDNA for *Fgfr2IIIb* (A,C,E,G) and *Fgfr1* (I,K) and sectioned in the transverse plane. A section taken through the otic region (the plane is indicated by a line through each embryo) is shown in the panel to the right of each whole embryo. Rostral is to the left. *Fgfr2IIIb* is expressed in the developing neurectoderm (n) at 3 (A,B), 6 (C,D), 8 (E,F) and 16 (G,H) somites. The onset of *Fgfr2IIIb* expression in the otic placode (op) coincides with placodal thickening (E,F) and persists to the otic cup (oc) stage (G,H). *Fgfr1* is expressed in the developing neurectoderm (n) from at least 4 (I,J) to 7 (K,L) somites. *Fgfr1* expression in the otic placode is apparent by 7 somites (K,L).

Table 1. Genotype data from *Fgf3*$^{+/-}$; *Fgf10*$^{+/-}$ intercross embryos harvested between E8.0 and E10.5

	Genotype								
	Fgf3$^{+/+}$; *Fgf10*$^{+/+}$	*Fgf3*$^{+/-}$; *Fgf10*$^{+/+}$	*Fgf3*$^{-/-}$; *Fgf10*$^{+/+}$	*Fgf3*$^{+/+}$; *Fgf10*$^{+/-}$	*Fgf3*$^{+/-}$; *Fgf10*$^{+/-}$	*Fgf3*$^{-/-}$; *Fgf10*$^{+/-}$	*Fgf3*$^{+/+}$; *Fgf10*$^{-/-}$	*Fgf3*$^{+/-}$; *Fgf10*$^{-/-}$	*Fgf3*$^{-/-}$; *Fgf10*$^{-/-}$
Expected number (total=1269)	79	58	79	158	317	158	79	158	79
Observed number	85	177	85	149	328	142	81	154	68

3A,C), characteristic of *Fgf10* and *Fgf3* single mutants, respectively (Mansour et al., 1993; Min et al., 1998; Sekine et al., 1999). Strikingly, the double mutant embryos also appeared to lack otic vesicles (Fig. 3C). Comparison of transverse sections of the control and double mutant embryos revealed bilateral microvesicles at the position expected for otic vesicles (Fig. 3B,D). Other double mutant embryos had either a unilateral microvesicle or lacked any sign of vesicle formation. Of 15 double mutant embryos, or 30 ears, analysed between E9.5 and E10.5, a microvesicle was identified in 15 cases (50%).

To determine the stage at which otic abnormalities initiated, embryos were harvested at progressively earlier times and otic development was analysed both morphologically and by using molecular markers (Fig. 3E-L, Fig. 4A-P). At E9.5, both *Pax2* (Fig. 3E,F) and *Dlx5* (Fig. 3I,J), which were expressed in control embryos in the ventromedial and dorsolateral wall of the otic vesicle respectively, were absent specifically from the otic region of double mutant embryos (Fig. 3G,H,K,L and data not shown), even when a microvesicle was present (Fig. 3H). These data show that otic development in double mutant embryos arrested prior to invagination of the otic cup to form the otic vesicle.

Fgf3$^{-/-}$; *Fgf10*$^{-/-}$ embryos lack the molecular features of a normal otic placode at E8.5

To determine whether the otic placode was induced correctly in embryos lacking both *Fgf3* and *Fgf10*, we analysed the morphology and expression patterns of four genes that mark the pre-placodal and placodal ectoderm in embryos with 6-10 somites (Fig. 4A-P). *Pax2* was expressed in the otic ectoderm of double heterozygote embryos with 8 somites (Fig. 4A,B). In

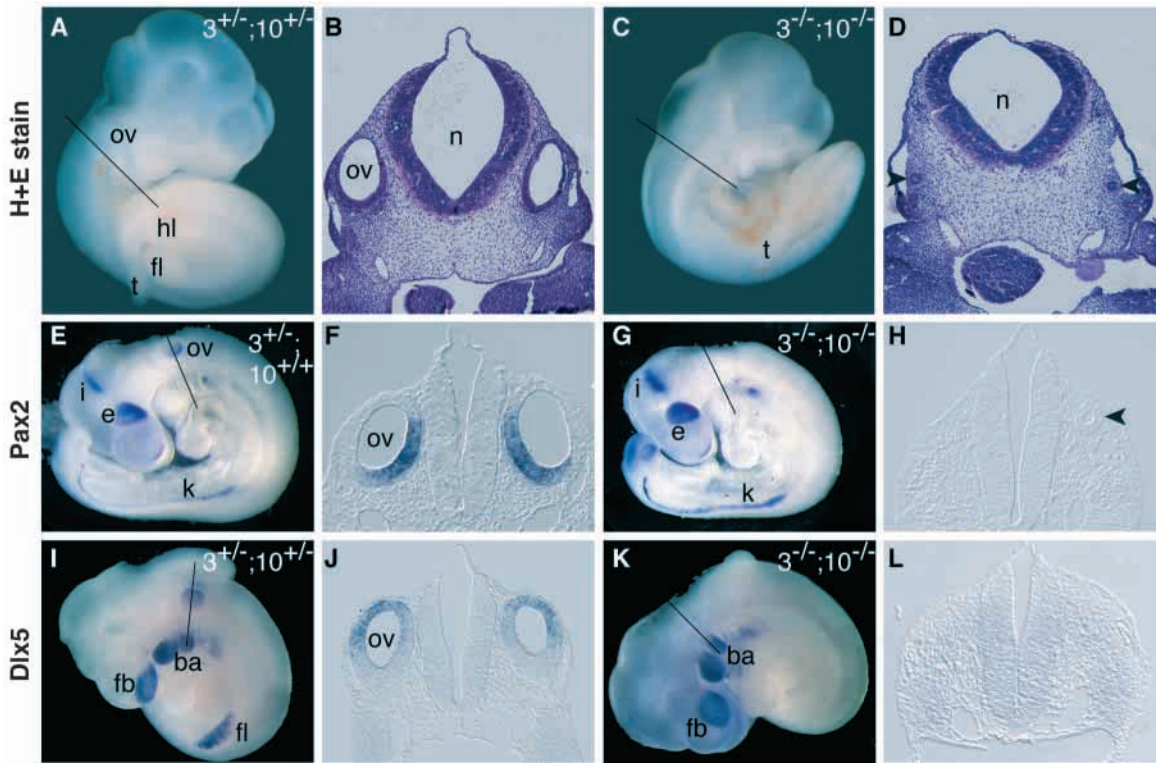

Fig. 3. Morphological and in situ hybridisation analyses of E9.5 and E10.5 *Fgf3/Fgf10* double mutant embryos reveal a failure of otic vesicle formation. Whole mount embryos were stained with haemotoxylin and eosin (A,C) or were probed with labelled cDNA for *Pax2* (E,G) and *Dlx5* (I,K) and sectioned in the transverse plane. A section taken through the otic region (the plane is indicated by a line through each embryo) is shown in the panel to the right of each whole embryo. Rostral is at the top (A,C) or to the left (E,G,I,K). Comparison of E10.5 control (A,B) and double mutant embryos (C,D) shows the absence of otic vesicles (ov), forelimbs (fl) and hindlimbs (hl) as well as truncation of the tail (t) in double mutants (C,D). In situ hybridisation with *Pax2* to E9.5 control (E) and double mutant (G) embryos detects transcripts in the eye (e), kidney (k) and isthmus (i). *Pax2* transcripts can be detected in the ventromedial wall of the otic vesicle in control embryos (F) but *Pax2* is absent from the comparable region of double mutant embryos (H). In situ hybridisation with *Dlx5* to E9.5 control (I) and double mutant (K) embryos detects transcripts in the first and second branchial arches (ba) and forebrain (f). *Dlx5* transcripts can be detected in the forelimb and the dorsolateral wall of the otic vesicle in control (I,J) but not double mutant (K,L) embryos. Arrowheads indicate microvesicles (D,H).

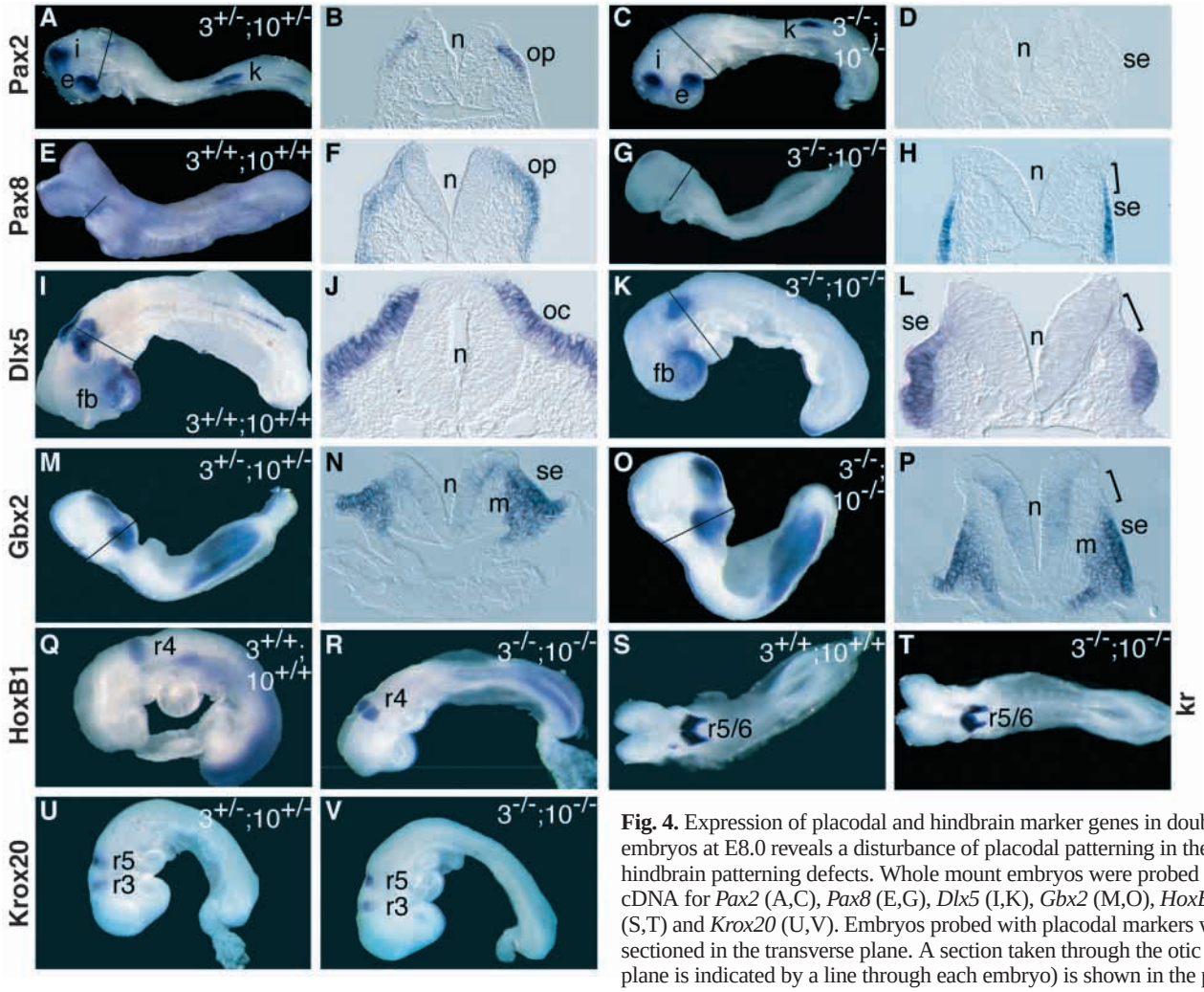

Fig. 4. Expression of placodal and hindbrain marker genes in double mutant embryos at E8.0 reveals a disturbance of placodal patterning in the absence of hindbrain patterning defects. Whole mount embryos were probed with labelled cDNA for *Pax2* (A,C), *Pax8* (E,G), *Dlx5* (I,K), *Gbx2* (M,O), *HoxB1* (Q,R), *kr* (S,T) and *Krox20* (U,V). Embryos probed with placodal markers were sectioned in the transverse plane. A section taken through the otic region (the plane is indicated by a line through each embryo) is shown in the panel to the right of each whole embryo. Rostral is to the left. In situ hybridisation with *Pax2* to 8 somite control (A) and double mutant (C) embryos detects transcripts in the eye (e), kidney (k) and isthmus (i). *Pax2* transcripts can be detected in the otic placode (op) in control (B) but not double mutant (D) embryos. At 8 somites, *Pax8* transcripts can be detected in control embryos in the otic placode and more ventrally in the surface ectoderm (F). In double mutant embryos, *Pax8* transcripts can only be detected in the more ventrally located surface ectoderm (se, H). In situ hybridisation with *Dlx5* to 10 somite control (I) and double mutant (K) embryos detects transcripts in the forebrain (fb). *Dlx5* transcripts can be detected in control embryos in the otic cup (oc) (J), but in double mutant embryos the region of *Dlx5* expressing thickened ectoderm is located more ventrally (L). At 6 somites, *Gbx2* is expressed throughout the surface ectoderm including the surface ectoderm and in the underlying mesoderm (m) (N). In double mutant embryos, *Gbx2* transcripts are excluded from the most dorsal regions of the surface ectoderm and from the underlying mesoderm of the otic region (P). At E9.0 *HoxB1*, *Mafb/kreisler* and *Krox20* are expressed in rhombomeres 4 (r4; Q), rhombomeres 5/6 (r5/6; S) and rhombomeres 3 and 5 (r3, r5; U), respectively. Expression of *HoxB1*, *Mafb/kreisler* and *Krox20* is unchanged in double mutant embryos (R,T,V). A bracket marks the location of the dorsal surface ectoderm of double mutant embryos, from which otic marker genes are excluded.

double mutant embryos, however, *Pax2* transcripts were absent specifically from the otic region (Fig. 4C,D). At 8 somites, *Pax8* was detected throughout the ectoderm lateral to r5 and r6 of wild-type embryos (Fig. 4E,F). In double mutant embryos, *Pax8* expression was restricted to ventral ectoderm and there was no placodal thickening in the dorsal ectoderm (Fig. 4G,H). In wild-type embryos with 10 somites, *Dlx5* was detected in the thickened otic ectoderm that was invaginating to form the otic cup (Fig. 4I,J). In double mutant embryos, expression of *Dlx5* was excluded from the dorsal surface ectoderm, which was unusually thin (Fig. 4K,L). There was, however, a region of *Dlx5*-expressing thickened ectoderm located more ventrally than that seen in the control (Fig. 4L). Interestingly, on one side of this embryo the region of thickened ectoderm appeared to be invaginating (Fig. 4L). *Gbx2* was expressed in the presumptive otic ectoderm and in a wedge of the underlying mesenchyme in 6-somite double heterozygote embryos (Fig. 4M,N). *Gbx2* expression in double mutant embryos, however, was excluded from the dorsal regions of both the ectoderm and mesenchyme (Fig. 4O,P). The abnormal morphology and absent or altered expression domains of all four otic marker genes in double mutant embryos suggest that correct induction of the otic placode requires both *Fgf3* and *Fgf10*.

Hindbrain patterning is not affected in *Fgf3*$^{-/-}$;*Fgf10*$^{-/-}$ embryos

Genes encoding FGF receptors, including *Fgfr2b*, are expressed in the developing hindbrain (Fig. 2 and data not

shown) (Yamaguchi et al., 1992) and FGFs play important roles in neural induction and patterning (Marin and Charnay, 2000). Indeed, zebrafish embryos depleted of both FGF3 and FGF8 have severe hindbrain patterning defects (Maves et al., 2002; Walshe et al., 2002). This raised the possibility that the otic defects we observed in *Fgf3/Fgf10* double mutants could be a secondary consequence of hindbrain abnormalities. To address this issue, we examined the expression patterns of three hindbrain marker genes, *Mafb/kreisler*, *HoxB1* and *Krox20*. As expected, double heterozygote control embryos at 9-13 somites expressed *HoxB1* in r4, *Mafb/kreisler* in r5 and r6 and *Krox20* in r3 and r5 (Fig. 4Q,S,U). Expression of these genes was unaffected in similarly staged double mutant embryos (Fig. 4R,T,V), suggesting that these embryos had grossly normal hindbrains. Furthermore, gross examination and microscopic observation of coronal sections of E9-10.5 double mutant embryos revealed normal rhombomeric divisions of the hindbrain (data not shown). Therefore, the abnormalities in otic development seen in double mutant embryos are probably a direct consequence of the loss of FGF3 and FGF10 signals to the otic ectoderm.

Cell proliferation and survival in the surface ectoderm of *Fgf3*$^{-/-}$;*Fgf10*$^{-/-}$ embryos are not significantly altered

Loss of both *Fgf3* and *Fgf10* clearly affects molecular patterning of the otic placode-forming region of the surface ectoderm. To determine whether there were additional effects of the loss of these two genes on cell proliferation, we labelled control and double mutant embryos at the 6 and 8 somite stages with an antibody directed against phosphohistone H3. No differences between embryos of different genotypes in the distribution of labelled cells were apparent upon examination of whole embryos. Furthermore, examination of cryosections from these embryos revealed that mitotic cells could be found in all tissues, including the dorsal region of the presumptive otic ectoderm, of both control and double mutant embryos (Fig. 5A-D). These data suggest that loss of *Fgf3* and *Fgf10* does not lead to a block in cell proliferation in these tissues. In addition, we investigated whether excessive cell death occurred in the tissues involved in otic development in double mutant embryos. Examination of TUNEL whole mount staining and cryosections revealed no major differences between 7 somite embryos of different genotypes in the number and distribution of apoptotic cells (Fig. 5E-H). Apoptotic cells could be found in all tissues of both control and double mutant embryos. Therefore, absence of both *Fgf3* and *Fgf10* was not associated with major changes in either mitogenic or survival signals within the otic region.

Fgf3 and *Fgf10* play quantitative and unequal roles in otic development

Observations of E9.5 *Fgf3*$^{-/-}$;*Fgf10*$^{+/-}$ and *Fgf3*$^{+/-}$;*Fgf10*$^{-/-}$ embryos suggested that these embryos had otic vesicle abnormalities that were distinguishable from each other and intermediate between those of *Fgf3*$^{-/-}$ or *Fgf10*$^{-/-}$ mutant embryos and those of double mutant embryos. To examine the morphology and patterning of these mutant vesicles, embryos with three mutant alleles were stained with *Pax2* and *Dlx5* and compared with the previously described control and double mutant embryos as well as with *Fgf3*$^{-/-}$ and *Fgf10*$^{-/-}$ embryos (Fig. 6). By comparison with control embryos (Fig. 3F,J) or with embryos homozygous for a single *Fgf* mutation (Fig. 6B,D,J,L), embryos with either combination of three mutant alleles appeared to have otic vesicles that were smaller (Fig. 6F,H,N,P). This phenotype was more extreme in the *Fgf3*$^{-/-}$;*Fgf10*$^{+/-}$ embryos (Fig. 6H,P) than in the *Fgf3*$^{+/-}$;*Fgf10*$^{-/-}$ embryos (Fig. 6F,N). Quantitative comparisons between the ratio of the area of the central otic vesicle section to the area of the central eye section in *Fgf3*$^{+/-}$;*Fgf10*$^{+/-}$, *Fgf3*$^{+/-}$;*Fgf10*$^{-/-}$ and *Fgf3*$^{-/-}$;*Fgf10*$^{+/-}$ embryos detected statistically significant differences between the three genotypes (Fig. 7A). The otic to optic area ratio of the *Fgf3*$^{+/-}$;*Fgf10*$^{-/-}$ and *Fgf3*$^{-/-}$;*Fgf10*$^{+/-}$ samples were approximately 72% (P=0.005) and 47% (P=0.001) respectively of that of the *Fgf3*$^{+/-}$;*Fgf10*$^{+/-}$ controls. As the otic vesicle is roughly spherical at this stage, these differences in area probably reflect even larger differences in volume.

We also observed an effect of the mutant *Fgf* alleles on the dorsal-ventral position of the otic vesicle. Some embryos

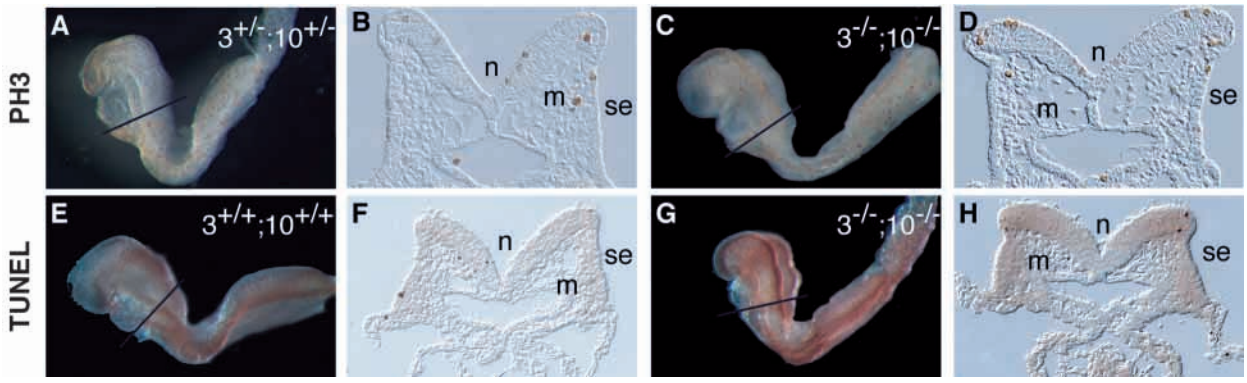

Fig. 5. Cell proliferation and survival are not altered significantly in *Fgf3*$^{-/-}$;*Fgf10*$^{-/-}$ embryos. Whole mount embryos were analysed for mitotic or apoptotic cells using an antibody to phosphohistone H3 (A,C) or TUNEL (E,G), respectively and sectioned in the transverse plane. A section taken through the otic region (the plane is indicated by a line through each embryo) is shown in the panel to the right of each whole embryo. Rostral is to the left. Phosphistone H3 immunoreactivity in transverse sections from an 8 somite control (B) and double mutant embryo (D). Mitotic cells (brown) can be identified in all three tissues that are involved in otic induction; neurectoderm (ne), mesoderm (m) and surface ectoderm (se). TUNEL staining in transverse sections from 7 somite control (F) and double mutant embryos (H). Apoptotic cells (brown) can be identified in all three tissues that are involved in otic induction; neurectoderm, mesoderm and surface ectoderm.

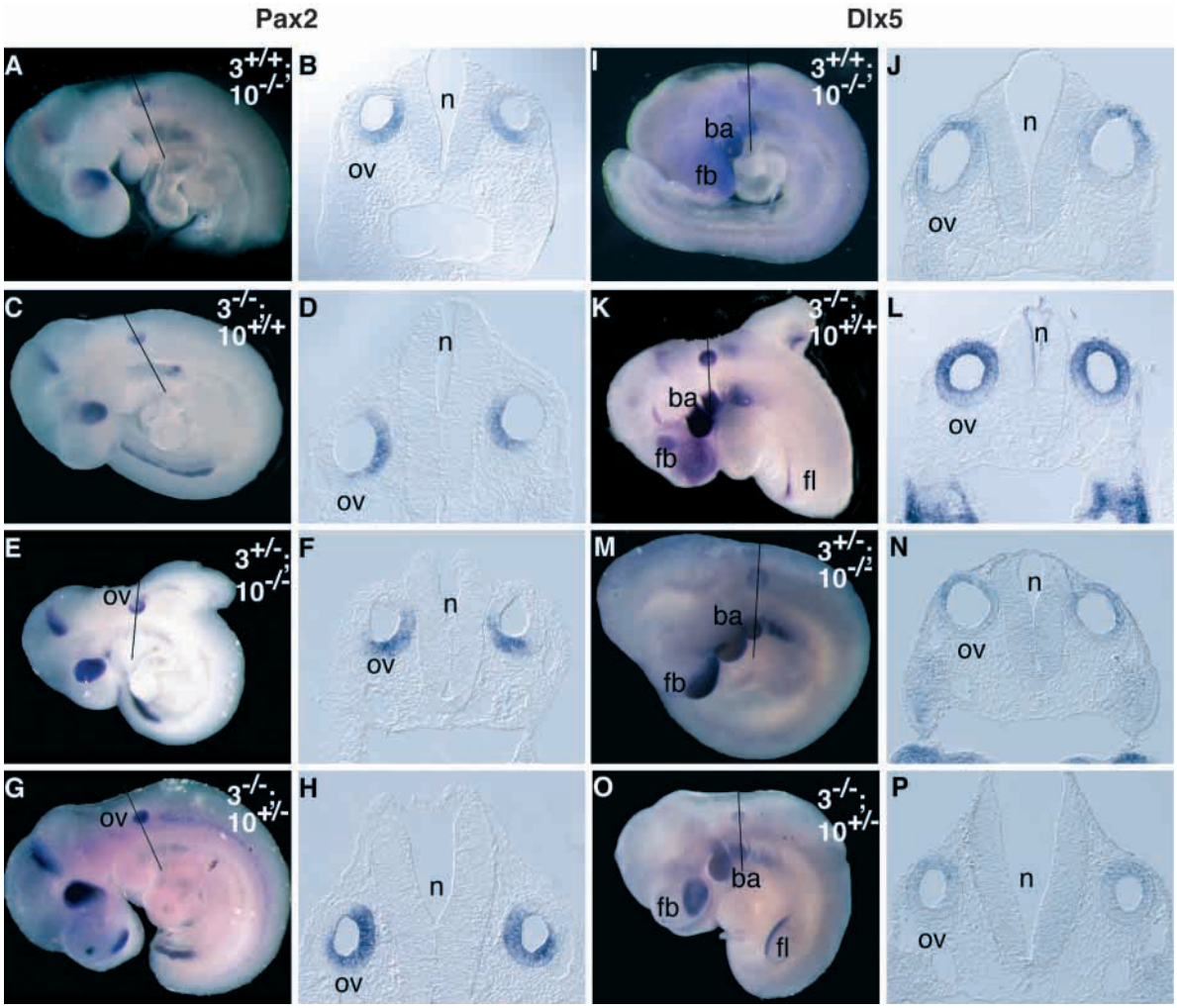

Fig. 6. *Pax2* and *Dlx5* expression in *Fgf3*$^{-/-}$ embryos, *Fgf10*$^{-/-}$ embryos and embryos with three mutant *Fgf* alleles reveals quantitative and unequal roles for *Fgf3* and *Fgf10* in otic development. Whole mount embryos were probed with labelled cDNA for *Pax2* (A,C,E,G) and *Dlx5* (I,K,M,O) and sectioned in the transverse plane. A section taken through the otic region (the plane is indicated by a line through each embryo) is shown in the panel to the right of each whole embryo. Rostral is to the left. The control and double mutant embryos for comparison are located in Fig. 3 and are shown at the same magnification. *Pax2* and *Dlx5* transcripts can be detected in the ventromedial (B,D,F,H) and dorsolateral (J,L,N,P) wall of the otic vesicle (ov), respectively. The size and location of the otic vesicle as well as the pattern of *Dlx5* expression are altered in *Fgf3*$^{-/-}$ mutants (D,L). In *Fgf3*$^{-/-}$;*Fgf10*$^{+/-}$ and *Fgf3*$^{+/-}$;*Fgf10*$^{-/-}$ embryos, the otic vesicles are reduced in size when compared to *Fgf3*$^{-/-}$ or *Fgf10*$^{-/-}$ embryos (F,H,N,P). In *Fgf3*$^{-/-}$;*Fgf10*$^{+/-}$ embryos (H,P), the otic vesicles are also located ventrally relative to the otic vesicles in *Fgf3*$^{-/-}$ (D,L) or *Fgf10*$^{-/-}$ (B,J) embryos and *Pax2* expression is expanded both dorsally and laterally (H). In embryos carrying either combination of three mutant alleles, *Dlx5* expression is reduced relative to that seen in the branchial arches (N,P).

homozygous only for the *Fgf3* mutation had otic vesicles that were more ventrally localised than those found in control embryos (Fig. 6D, Fig. 3F). This observation is consistent with the previously described variable expressivity of the *Fgf3*$^{-/-}$ otic phenotype, but was not quantified because of its variability (Mansour et al., 1993). The ventralised location of the otic vesicle was more extreme and less variable in the *Fgf3*$^{-/-}$;*Fgf10*$^{+/-}$ embryos (Fig. 6H,P) than in the *Fgf3*$^{-/-}$;*Fgf10*$^{+/+}$ embryos (Fig. 6F,N). To quantify this observation, the distance from the dorsal surface of the neural tube to the top of the otic vesicle was measured and compared to the dorsoventral length of the neural tube in sections prepared from *Fgf3*$^{+/-}$;*Fgf10*$^{+/-}$, *Fgf3*$^{+/-}$;*Fgf10*$^{-/-}$ and *Fgf3*$^{-/-}$;*Fgf10*$^{+/-}$ embryos. (Fig. 7B). By this measure, the position of the otic vesicle in *Fgf3*$^{-/-}$;*Fgf10*$^{+/-}$ embryos was significantly ventralised relative to that in *Fgf3*$^{+/-}$;*Fgf10*$^{+/-}$ embryos (P=0.001). No significant differences, however, could be detected between the positions of the otic vesicles in *Fgf3*$^{+/-}$;*Fgf10*$^{-/-}$ and *Fgf3*$^{+/-}$;*Fgf10*$^{+/-}$ embryos.

Alterations in otic marker gene expression were also apparent in these E9.5 embryos. Whereas the localisation of *Pax2* to the ventromedial region of the otic vesicle was similar in control (Fig. 3F), *Fgf3*$^{+/+}$;*Fgf10*$^{-/-}$ (Fig. 6B), *Fgf3*$^{-/-}$;*Fgf10*$^{+/+}$ (Fig. 6D) and in *Fgf3*$^{+/-}$;*Fgf10*$^{-/-}$ (Fig. 6F) embryos, *Pax2* otic expression expanded both dorsally and laterally in *Fgf3*$^{-/-}$;*Fgf10*$^{+/-}$ embryos (Fig. 6H). *Dlx5*

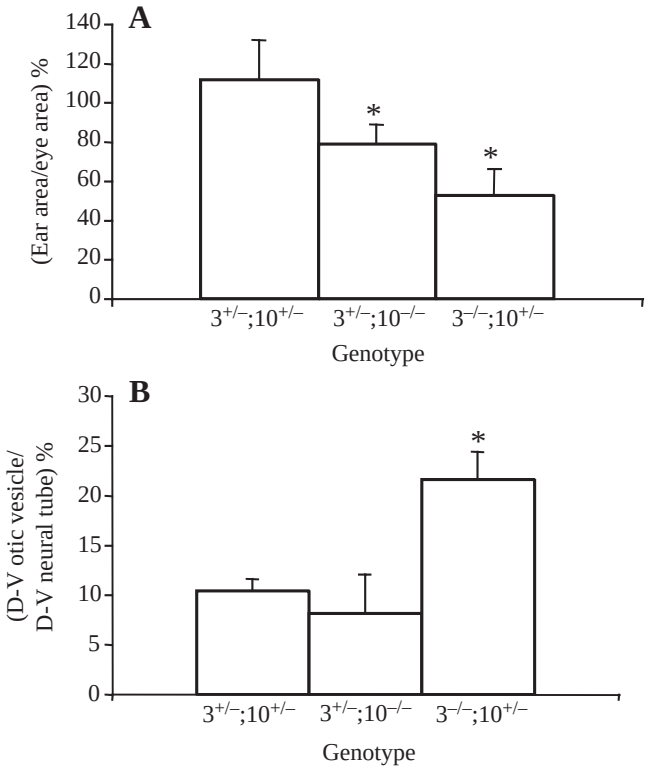

Fig. 7. Analysis of the area and position of the otic vesicle in embryos with three mutant *Fgf* alleles reveals quantitative differences between *Fgf3*$^{+/-}$;*Fgf10*$^{-/-}$ and *Fgf3*$^{-/-}$;*Fgf10*$^{+/-}$ embryos. (A) Quantitative comparisons between the ratio of the area of the central otic vesicle section to the area of the central eye section in *Fgf3*$^{+/-}$;*Fgf10*$^{+/-}$, *Fgf3*$^{+/-}$;*Fgf10*$^{-/-}$ and *Fgf3*$^{-/-}$;*Fgf10*$^{+/-}$ embryos (n=6 ears and eyes per genotype). The average ear area/eye area (in %) is shown on the *y*-axis. The genotypes analysed are shown on the *x*-axis. The otic to optic area ratios of the *Fgf3*$^{+/-}$;*Fgf10*$^{-/-}$ and *Fgf3*$^{-/-}$;*Fgf10*$^{+/-}$ samples were significantly lower than that of the *Fgf3*$^{+/-}$;*Fgf10*$^{+/-}$ embryos (P=0.005 and P=0.001, respectively). (B) Quantitative analysis of the dorsal-ventral position of the otic vesicle. The vertical distance from the dorsal surface of the neural tube to the top of the otic vesicle was measured and compared to the dorsoventral length of the neural tube in *Fgf3*$^{+/-}$;*Fgf10*$^{+/-}$, *Fgf3*$^{+/-}$;*Fgf10*$^{-/-}$, and *Fgf3*$^{-/-}$;*Fgf10*$^{+/-}$ embryos (n=6 ears per genotype). The dorsoventral (DV) distance to the otic vesicle/dorsoventral length of the neural tube is shown on the *y*-axis. The genotypes analysed are shown on the *x*-axis. The position of the otic vesicle in *Fgf3*$^{-/-}$;*Fgf10*$^{+/-}$ embryos was significantly ventralised relative to that in *Fgf3*$^{+/-}$;*Fgf10*$^{+/-}$ embryos (P=0.001). The asterisk indicates a significant paired *t* test result between the genotype shown and *Fgf3*$^{+/-}$;*Fgf10*$^{+/-}$ embryos. The bar above each data cell indicates one s.d. 3, *Fgf3*; 10, *Fgf10*.

expression was found in the dorsolateral region of otic vesicles of all combinations of *Fgf* mutant genotypes (Fig. 3J, Fig. 6J,L,N,P) except the double mutant, which does not have otic vesicles. In addition, there appears to be an expansion of *Dlx5* towards the ventral and medial regions of the otic vesicle in the *Fgf3*$^{-/-}$;*Fgf10*$^{+/+}$ embryo (Fig. 6L). Compared with control embryos (Fig. 3J), the level of *Dlx5* expression in the otic vesicle relative to that seen in the branchial arches, forebrain and limbs appeared markedly reduced in *Fgf3*$^{+/-}$;*Fgf10*$^{-/-}$ and *Fgf3*$^{-/-}$;*Fgf10*$^{+/-}$ embryos (Fig. 6N,P). This reduced level of *Dlx5* expression made it difficult to determine whether the domain of expression was altered. Taken together, these data suggest that there is a quantitative requirement for FGF signalling to promote normal otic development and that loss of FGF3 has a more significant effect on otic development than does loss of FGF10.

DISCUSSION

The absence of otic vesicles and abnormalities of otic placode marker gene expression in the *Fgf3*/*Fgf10* double mutant embryos argue that these two genes are required for otic placode induction. This dual requirement explains why no classic or single gene targeted mouse mutants that lack inner ears have ever been described. The functional redundancy exhibited by *Fgf3* and *Fgf10* in early otic development is not a simple matter of co-expression of the two *Fgf* genes in the same inducing tissue, as their expression patterns change dynamically during otic placode induction and only coincide for a brief time in the hindbrain, after the placode has begun to invaginate. Taking our data together with the tissue requirements for otic placode induction, we suggest that the FGF signalling required for normal otic placode induction has two sources, FGF10 expressed by the mesenchyme underlying the entire prospective otic ectoderm, and FGF3, expressed in the caudal hindbrain. The proposed role for *Fgf10* in the mouse might therefore be analogous to that proposed for mesodermal FGF19 in the chick (Ladher et al., 2000).

We found that in *Fgf3/Fgf10* double mutant embryos at E8.5, all tested markers of prospective otic ectoderm were either entirely eliminated from the ectoderm (*Pax2*), or were excluded from the dorsal ectoderm (*Dlx5*, *Gbx2* and *Pax8*). In contrast, it did not appear that cell proliferation or survival in the otic ectoderm of double mutant embryos was significantly affected. Taken together, these results suggest that the main role of FGF signalling in otic induction is to establish appropriate patterns of gene expression in dorsal ectoderm. These data are consistent with the finding that zebrafish *Dlx5* responds to signals required for placodal induction (Solomon and Fritz, 2002). This role is different from that proposed for FGF signalling in the development of the midbrain, in which *Fgf8* and *Fgf17* are required quantitatively to regulate cell proliferation (Xu et al., 2000). The role of *Fgf3* and *Fgf10* in otic development also differs from that of *Fgf8* in neural crest development (Abu-Issa et al., 2002; Frank et al., 2002) and of *Fgf4* and *Fgf8* in limb development (Sun et al., 2002), in which the respective signals are required for cell survival.

Although the double mutant otic phenotype was fully penetrant, there remains some variable expressivity, as microvesicles were observed lateral to the hindbrain in 50% of cases between E9.5 and E10.5. None of the microvesicles expressed otic markers, suggesting that they are not likely to develop similarly to bona fide inner ears. Our observation, however, of a ventrally localised thickening of the ectoderm in some E8.5 double mutant embryos, accompanied in one case by a small invagination, which may be a precursor of a microvesicle, does suggest that double mutant embryos may still express a weak signal with vesicle-inducing properties. Whether this signal is an additional FGF normally involved in

otic induction or another type of signal remains to be determined.

FGF3 and FGF10 are likely to induce ear development in a paracrine fashion through their high-affinity receptor FGFR2b, the transcript for which is first detectable in the prospective otic placode at approximately the eight-somite stage. The simplest model for otic induction that is consistent with all of the data is that FGF3 expressed from the hindbrain and FGF10 expressed from the mesenchyme act directly to activate FGFR2b in the ectoderm. It could be argued, however, that the timing of receptor gene expression in the ectoderm is slightly later than might be expected if FGF signalling were the primary means by which the ectoderm is induced. In avians, otic placode specification is thought to be complete by the 4-6 somite stage and this cranial ectoderm is committed to an otic fate by the 10 somite stage (Groves and Bronner-Fraser, 2000). In mice, however, prior to the present studies, the timing of otic induction had not been established by any criteria other than that of placodal thickening, which in different accounts has been reported to occur between 4 and 13 somites (Anniko and Wikstrom, 1984; Sulik and Cotanche, 1995; Rinkwitz et al., 2001; Kiernan et al., 2002). Our own observations suggest that thickening occurs between 7 and 8 somites (this report and T.J.W. and S.L.M., unpublished). Thus it is possible that otic induction occurs slightly later in mice than in other species. Furthermore, the in situ hybridisation method for detecting *Fgfr* gene expression may not be sensitive enough to indicate the true onset of FGF signalling in the ectoderm, which could occur as soon as the first receptor transcripts are translated and the receptor is inserted within the cell membrane, but before the *Fgfr* transcripts accumulate to levels detectable by in situ hybridisation.

More complex models for FGF3 and FGF10 function in otic placode induction cannot be excluded at this time. For example, it is possible that FGF10, expressed in early somite stage mesenchyme, has two functions. It could signal first to FGFR2b in the hindbrain, activating *Fgf3* expression, and later signal in combination with hindbrain FGF3 to FGFR2b in the ectoderm. At this point it is unclear whether the FGF3 expressed in the prospective placode itself also plays an important autocrine-signalling role. Tissue-specific ablation of *Fgf3* will be required to address this point.

It is curious that the otic abnormalities of embryos lacking *Fgfr2b* or expressing a dominant negative FGF receptor are much less severe than those of the double ligand mutants described here. Embryos homozygous for an *Fgfr2b* isoform-specific targeted deletion or heterozygous for a secreted dominant negative form of FGFR2b have small otic vesicles at E10 and E11 (Celli et al., 1998; Pirvola et al., 2000). One possible explanation for the milder otic phenotypes displayed by these mutant embryos is that there may be some redundancy at the level of the placodal receptor that is provided by FGFR1b, the only other FGF receptor thought to be activated by FGF3 and FGF10 (Ornitz et al., 1996; Beer et al., 2000). Consistent with this possibility, we find that there is some detectable expression of *Fgfr1*, probably encoding the IgIIIb isoform, at the time when the otic ectoderm assumes a placodal morphology. When FGFR2b is absent or inhibited, it is possible that the low levels of FGFR1b could weakly transduce the FGF3 and FGF10 otic-inducing signals.

A different *Fgf*, *Fgf8*, has been shown to be required redundantly with *Fgf3* for otic placode induction in zebrafish (Phillips et al., 2001; Leger and Brand, 2002; Maroon et al., 2002). In this case, however, the severe abnormalities of hindbrain patterning (Phillips et al., 2001; Maroon et al., 2002; Maves et al., 2002; Walshe et al., 2002) argue that FGF8 may not act directly on the prospective otic placode, which does not express its highest affinity receptor, FGFR4 (Ornitz et al., 1996), but may instead act indirectly through the hindbrain, which does express FGFR4 (T.J. Wright and S.L. Mansour, unpublished). An alternative explanation that does not exclude the first possibility is that FGF8 functions very early in gastrulation on the mesoderm, and in its absence, the mesoderm is reduced and/or does not express otic-inducing signals such as FGF10. A final possibility is that there are species-specific differences in FGF identity and their sites of action with respect to otic placode development. Studies of mouse *Fgf3/Fgf8* mutant combinations may help to address this point.

The otic phenotypes identified in mice carrying three mutant alleles suggest that there is a quantitative requirement for FGF signalling to promote normal otic development and that loss of *Fgf3* is more detrimental than loss of *Fgf10*. In particular, in the absence of *Fgf3*, genes with polarised domains of expression in the otic vesicle become less polarised, whereas in the absence of *Fgf10*, polarised expression appears to be maintained. This effect might be explained if the otic placode experiences a dorsal (high) to ventral (low) gradient of FGF3 expressed from the hindbrain. In contrast, the primary source of FGF10 is the mesenchyme underlying the entire placode, and these cells may experience a constant concentration of FGF10. This difference may explain why failure of endolymphatic duct outgrowth, a dorsal structure, is the primary defect in *Fgf3* single mutants (Mansour et al., 1993), whereas this process occurs normally in *Fgf10* single mutants (Ohuchi et al., 2000). It would be interesting to determine the effects of reversing the proposed FGF3 gradient.

We are grateful for helpful discussions and prepublication data supplied by Drs Philippa Francis-West, Bernd Fritzsch, Raj Ladher, Gary Schoenwolf and Lisa Maves. We thank Dr Scott Simonet for permission to use the *Fgf10* mutant strain and Dr David Ornitz for sending it to us. cDNA clones were generously shared by John Rubenstein (*Dlx5*), Peter Gruss (*Pax2*, *Pax8*), Gail Martin (*Gbx2*), Paivi Kettunen (*Fgfr2b*), Mario Cappechi (*HoxB1*, *kr*, *Krox20*) and David Ornitz (*Fgf10*). Technical assistance was provided by Ekaterina Hatch. The manuscript was improved by helpful comments from Drs Capecchi, Schoenwolf and Thummel. This work was supported by grants from the Deafness Research Foundation (T.J.W.) and the NIDCD (DC00473 to T.J.W. and DC04185 to S.L.M.).

REFERENCES

Abu-Issa, R., Smyth, G., Smoak, I., Yamamura, K. and Meyers, E. N. (2002). Fgf8 is required for pharyngeal arch and cardiovascular development in the mouse. *Development* **129**, 4613-4625.

Adamska, M., Herbrand, H., Adamski, M., Kruger, M., Braun, T. and Bober, E. (2001). FGFs control the patterning of the inner ear but are not able to induce the full ear program. *Mech. Dev.* **109**, 303-313.

Anniko, M. and Wikstrom, S. O. (1984). Pattern formation of the otic placode and morphogenesis of the otocyst. *Am. J. Otol.* **5**, 373-381.

Baker, C. V. and Bronner-Fraser, M. (2001). Vertebrate cranial placodes I. Embryonic induction. *Dev. Biol.* **232**, 1-61.

Beer, H. D., Vindevoghel, L., Gait, M. J., Revest, J. M., Duan, D. R.,

Mason, I., Dickson, C. and Werner, S. (2000). Fibroblast growth factor (FGF) receptor 1-IIIb is a naturally occurring functional receptor for FGFs that is preferentially expressed in the skin and the brain. *J. Biol. Chem.* **275**, 16091-16097.

Carpenter, E. M., Goddard, J. M., Chisaka, O., Manley, N. R. and Capecchi, M. R. (1993). Loss of *Hox-A1* (*Hox-1.6*) function results in the reorganization of the murine hindbrain. *Development* **118**, 1063-1075.

Celli, G., LaRochelle, W. J., Mackem, S., Sharp, R. and Merlino, G. (1998). Soluble dominant-negative receptor uncovers essential roles for fibroblast growth factors in multi-organ induction and patterning. *EMBO J.* **17**, 1642-1655.

Cordes, S. P. and Barsh, G. S. (1994). The mouse segmentation gene *kr* encodes a novel basic domain-leucine zipper transcription factor. *Cell* **79**, 1025-1034.

Crossley, P. H. and Martin, G. R. (1995). The mouse *Fgf8* gene encodes a family of polypeptides and is expressed in regions that direct outgrowth and patterning in the developing embryo. *Development* **121**, 439-451.

Depew, M. J., Liu, J. K., Long, J. E., Presley, R., Meneses, J. J., Pedersen, R. A. and Rubenstein, J. L. (1999). Dlx5 regulates regional development of the branchial arches and sensory capsules. *Development* **126**, 3831-3846.

Dressler, G. R., Deutsch, U., Chowdhury, K., Nornes, H. O. and Gruss, P. (1990). *Pax2*, a new murine paired-box-containing gene and its expression in the developing excretory system. *Development* **109**, 787-795.

Frank, D. U., Fotheringham, L. K., Brewer, J. A., Muglia, L. J., Tristani-Firouzi, M., Capecchi, M. R. and Moon, A. M. (2002). An Fgf8 mouse mutant phenocopies human 22q11 deletion syndrome. *Development* **129**, 4591-4603.

Frohman, M. A., Martin, G. R., Cordes, S. P., Halamek, L. P. and Barsh, G. S. (1993). Altered rhombomere-specific gene expression and hyoid bone differentiation in the mouse segmentation mutant, *kreisler* (*kr*). *Development* **117**, 925-936.

Gavalas, A., Trainor, P., Ariza-McNaughton, L. and Krumlauf, R. (2001). Synergy between Hoxa1 and Hoxb1: the relationship between arch patterning and the generation of cranial neural crest. *Development* **128**, 3017-3027.

Graham, A. (1999). Whole embryo assays for programmed cell death. In *Molecular Embryology, Methods and Protocols* (ed. P. T. Sharpe and I. Mason), pp. 667-672. Totowa, NJ: Humana Press.

Groves, A. K. and Bronner-Fraser, M. (2000). Competence, specification and commitment in otic placode induction. *Development* **127**, 3489-3499.

Henrique, D., Adam, J., Myat, A., Chitnis, A., Lewis, J. and Ish-Horowicz, D. (1995). Expression of a Delta homologue in prospective neurons in the chick. *Nature* **375**, 787-790.

Igarashi, M., Finch, P. W. and Aaronson, S. A. (1998). Characterization of recombinant human fibroblast growth factor (FGF)-10 reveals functional similarities with keratinocyte growth factor (FGF-7). *J. Biol. Chem.* **273**, 13230-13235.

Kettunen, P., Karavanova, I. and Thesleff, I. (1998). Responsiveness of developing dental tissues to fibroblast growth factors: expression of splicing alternatives of FGFR1, -2, -3, and of FGFR4; and stimulation of cell proliferation by FGF-2, -4, -8, and -9. *Dev. Genet.* **22**, 374-385.

Kiernan, A. E., Steel, K. P. and Fekete, D. M. (2002). Development of the mouse inner ear. In *Mouse Development: Patterning Morphogenesis and Organogenesis* (ed. J. Rossant and P. Tam), pp. 539-566. San Diego, CA, USA: Academic Press.

Ladher, R. K., Anakwe, K. U., Gurney, A. L., Schoenwolf, G. C. and Francis-West, P. H. (2000). Identification of synergistic signals initiating inner ear development. *Science* **290**, 1965-1967.

Leger, S. and Brand, M. (2002). Fgf8 and Fgf3 are required for zebrafish ear placode induction, maintenance and inner ear patterning. *Mech. Dev.* **119**, 91-108.

Maden, M., Graham, A., Gale, E., Rollinson, C. and Zile, M. (1997). Positional apoptosis during vertebrate CNS development in the absence of endogenous retinoids. *Development* **124**, 2799-2805.

Mahmood, R., Kiefer, P., Guthrie, S., Dickson, C. and Mason, I. (1995). Multiple roles for FGF-3 during cranial neural development in the chicken. *Development* **121**, 1399-1410.

Mahmood, R., Mason, I. J. and Morriss-Kay, G. M. (1996). Expression of *Fgf-3* in relation to hindbrain segmentation, otic pit position and pharyngeal arch morphology in normal and retinoic acid-exposed mouse embryos. *Anat. Embryol.* **194**, 13-22.

Manley, N. R. and Capecchi, M. R. (1995). The role of Hoxa-3 in mouse thymus and thyroid development. *Development* **121**, 1989-2003.

Mansour, S. L., Goddard, J. M. and Capecchi, M. R. (1993). Mice homozygous for a targeted disruption of the proto-oncogene *int-2* have developmental defects in the tail and inner ear. *Development* **117**, 13-28.

Marin, F. and Charnay, P. (2000). Hindbrain patterning: FGFs regulate Krox20 and mafB/kr expression in the otic/preotic region. *Development* **127**, 4925-4935.

Maroon, H., Walshe, J., Mahmood, R., Kiefer, P., Dickson, C. and Mason, I. (2002). Fgf3 and Fgf8 are required together for formation of the otic placode and vesicle. *Development* **129**, 2099-2108.

Maves, L., Jackman, W. and Kimmel, C. B. (2002). FGF3 and FGF8 mediate a rhombomere 4 signaling activity in the zebrafish hindbrain. *Development* **129**, 3825-3837.

McKay, I. J., Lewis, J. and Lumsden, A. (1996). The role of FGF-3 in early inner ear development: an analysis in normal and *kreisler* mutant mice. *Dev. Biol.* **174**, 370-378.

McKay, I. J., Muchamore, I., Krumlauf, R., Maden, M., Lumsden, A. and Lewis, J. (1994). The *kreisler* mouse: a hindbrain segmentation mutant that lacks two rhombomeres. *Development* **120**, 2199-2211.

McMahon, A., O'Neill, L. and Carroll, J. (1990). Proteolysis of the zona pellucida of mouse ova. *Biochem. Soc. Trans.* **18**, 340-341.

Min, H., Danilenko, D. M., Scully, S. A., Bolon, B., Ring, B. D., Tarpley, J. E., DeRose, M. and Simonet, W. S. (1998). Fgf-10 is required for both limb and lung development and exhibits striking functional similarity to *Drosophila branchless*. *Genes Dev.* **12**, 3156-3161.

Moens, C. B., Cordes, S. P., Giorgianni, M. W., Barsh, G. S. and Kimmel, C. B. (1998). Equivalence in the genetic control of hindbrain segmentation in fish and mouse. *Development* **125**, 381-391.

Noramly, S. and Grainger, R. M. (2002). Determination of the embryonic inner ear. *J. Neurobiol.* **53**, 100-128.

Ohuchi, H., Hori, Y., Yamasaki, M., Harada, H., Sekine, K., Kato, S. and Itoh, N. (2000). FGF10 acts as a major ligand for FGF receptor 2 IIIb in mouse multi-organ development. *Biochem. Biophys. Res. Commun.* **277**, 643-649.

Ornitz, D. M. and Itoh, N. (2001). Fibroblast growth factors. *Genome Biol.* **2**, 3005.1-3005.12.

Ornitz, D. M., Xu, J., Colvin, J. S., McEwen, D. G., MacArthur, C. A., Coulier, F., Gao, G. and Goldfarb, M. (1996). Receptor specificity of the fibroblast growth factor family. *J. Biol. Chem.* **271**, 15292-15297.

Orr-Urtreger, A., Bedford, M. T., Burakova, T., Arman, E., Zimmer, Y., Yayon, A., Givol, D. and Lonai, P. (1993). Developmental localization of the splicing alternatives of fibroblast growth factor receptor-2 (FGFR2). *Dev. Biol.* **158**, 475-486.

Pauley, S., Wright, T. J., Pirvola, U., Ornitz, D. M., Beisel, K. W. and Fritzsch, B. (2003). Expression and function of FGF10 in mammalian inner ear development. *Dev. Dyn.* **227**, 203-215.

Phillips, B. T., Bolding, K. and Riley, B. B. (2001). Zebrafish fgf3 and fgf8 encode redundant functions required for otic placode induction. *Dev. Biol.* **235**, 351-365.

Pirvola, U., Spencer-Dene, B., Xing-Qun, L., Kettunen, P., Thesleff, I., Fritzsch, B., Dickson, C. and Ylikoski, J. (2000). FGF/FGFR-2(IIIb) signaling is essential for inner ear morphogenesis. *J. Neurosci.* **20**, 6125-6134.

Plachov, D., Chowdhury, K., Walther, C., Simon, D., Guenet, J. L. and Gruss, P. (1990). Pax8, a murine paired box gene expressed in the developing excretory system and thyroid gland. *Development* **110**, 643-651.

Represa, J., Leon, Y., Miner, C. and Giraldez, F. (1991). The *int-2* proto-oncogene is responsible for induction of the inner ear. *Nature* **353**, 561-563.

Rinkwitz, S., Bober, E. and Baker, R. (2001). Development of the vertebrate inner ear. *Ann. New York Acad. Sci.* **942**, 1-14.

Sekine, K., Ohuchi, H., Fujiwara, M., Yamasaki, M., Yoshizawa, T., Sato, T., Yagishita, N., Matsui, D., Koga, Y. and Itoh, N. et al. (1999). Fgf10 is essential for limb and lung formation. *Nat. Genet.* **21**, 138-141.

Solomon, K. S. and Fritz, A. (2002). Concerted action of two dlx paralogs in sensory placode formation. *Development* **129**, 3127-3136.

Stark, M. R., Biggs, J. J., Schoenwolf, G. C. and Rao, M. S. (2000). Characterization of avian frizzled genes in cranial placode development. *Mech. Dev.* **93**, 195-200.

Sulik, K. K. and Cotanche, D. A. (1995). Embryology of the ear. In *Hereditary Hearing Loss and its Syndromes* (ed. R. J. Gorlin, H. V. Toriello and M. M. Cohen), pp. 22-42. Oxford, UK: Oxford University Press.

Sun, X., Mariani, F. V. and Martin, G. R. (2002). Functions of FGF signalling from the apical ectodermal ridge in limb development. *Nature* **418**, 501-508.

Sun, X., Meyers, E. N., Lewandoski, M. and Martin, G. R. (1999). Targeted

disruption of Fgf8 causes failure of cell migration in the gastrulating mouse embryo. *Genes Dev.* **13**, 1834-1846.

Torres, M. and Giraldez, F. (1998). The development of the vertebrate inner ear. *Mech. Dev.* **71**, 5-21.

Vendrell, V., Carnicero, E., Giraldez, F., Alonso, M. T. and Schimmang, T. (2000). Induction of inner ear fate by FGF3. *Development* **127**, 2011-2019.

Walshe, J., Maroon, H., McGonnell, I. M., Dickson, C. and Mason, I. (2002). Establishment of hindbrain segmental identity requires signaling by FGF3 and FGF8. *Curr. Biol.* **12**, 1117-1123.

Wassarman, K. M., Lewandoski, M., Campbell, K., Joyner, A. L., Rubenstein, J. L., Martinez, S. and Martin, G. R. (1997). Specification of the anterior hindbrain and establishment of a normal mid/hindbrain organizer is dependent on Gbx2 gene function. *Development* **124**, 2923-2934.

Wilkinson, D. G., Peters, G., Dickson, C. and McMahon, A. P. (1988). Expression of the FGF-related proto-oncogene *int-2* during gastrulation and neurulation in the mouse. *EMBO J.* **7**, 691-695.

Xu, J., Liu, Z. and Ornitz, D. M. (2000). Temporal and spatial gradients of Fgf8 and Fgf17 regulate proliferation and differentiation of midline cerebellar structures. *Development* **127**, 1833-1843.

Xu, X., Weinstein, M., Li, C., Naski, M., Cohen, R. I., Ornitz, D. M., Leder, P. and Deng, C. (1998). Fibroblast growth factor receptor 2 (FGFR2)-mediated reciprocal regulation loop between FGF8 and FGF10 is essential for limb induction. *Development* **120**, 753-765.

Yamaguchi, T. P., Conlon, R. A. and Rossant, J. (1992). Expression of the fibroblast growth factor receptor FGFR-1/flg during gastrulation and segmentation in the mouse embryo. *Dev. Biol.* **152**, 75-88.